Wave Simulation in the Outer Río de la Plata Estuary: Evaluation of SWAN Model

W. C. Dragani[1]; E. Garavento[2]; C. G. Simionato[3]; M. N. Nuñez[4]; P. Martin[5]; and M. I. Campos[6]

Abstract: This work discusses the implementation and validation of the SWAN model forced by NCEP/NCAR reanalyzed 10 m winds in the outer Río de la Plata (RDP) and adjacent continental shelf that will be used to study the wave climate in the region. Thirteen-month-long in situ data series of wave parameters are used to validate the results from numerical simulations. A set of numerical experiments is carried out in order to find a suitable computational domain to generate realistic simulations in the mouth of the RDP estuary. Numerical experiments including current and sea level fields are run, demonstrating that simulated wave parameters at the outer RDP are not significantly improved. A correction coefficient, dependent on wind speed, is applied to the wind drag factor in order to minimize the differences between simulated and observed wave parameters. The relatively low resolution wave model that satisfactorily simulates in situ wave heights and directions but slightly underestimates periods is a reliable tool for future applications and investigations.

DOI: 10.1061/(ASCE)0733-950X(2008)134:5(299)

CE Database subject headings: Simulation; Estuaries; Forecasting; Ocean waves; Parameters.

Introduction

Although a modern wave forecast system is available for the Atlantic Ocean (http://polar.ncep.noaa.gov/waves/main-table.html) and several local efforts are being carried out by the Servicio de Hidrografía Naval of Argentina to develop a wave forecast system, a wave climate is not available for the Río de la Plata (RDP) and the adjacent continental shelf (Fig. 1). There are four possible wave data sources to build a wave climate: (1) altimeter measurements from ERS-1, ERS-2, and TOPEX instruments (Cotton and Carter 1994; Woolf et al. 2002); (2) voluntary observing ships (VOS) (Gulev et al. 2003, Wilkerson and Earle 1990); (3) in situ observations; and (4) wave model hindcasts (Sterl et al. 1998, Cox and Swail 2001). Even though the first two provide global coverage, data quality has serious limitations. Waves derived from altimetry are dependent on the retrieval algorithms applied and are not available at very shallow coastal waters, as is the case for the intermediate and upper RDP. Significant wave heights estimated from altimeter-derived data have a precision of 0.5 m or 10% (Dobson et al. 1987), and VOS waves, being visual measurements, are quite inaccurate. Given that there is only one location in the outer RDP (Fig. 1) where direct measurements were gath-

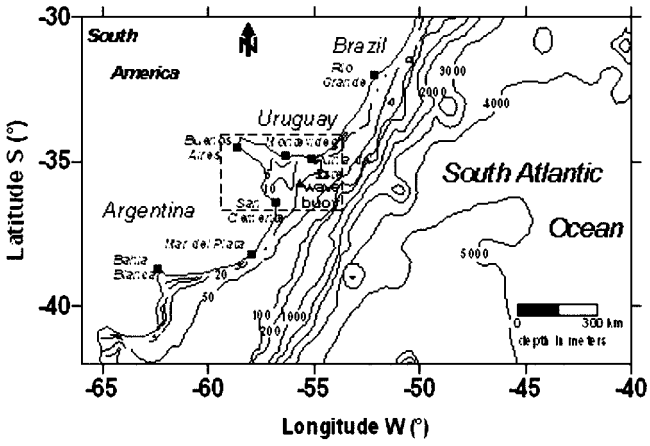

Fig. 1. RDP and adjacent continental shelf: computational domains tested in the SWAN model. Smallest model domain used in numerical experiments is indicated with dashed lines. Depth contours in meters; the 200 m depth contour is highlighted with a heavy line.

[1]Centro de Investigaciones del Mar y la Atmósfera (CIMA/CONICET-UBA), Ciudad Universitaria, Pabellón II, 2do. Piso. (C1428EGA) Ciudad Autónoma de Buenos Aires, Argentina.

[2]Centro de Investigaciones del Mar y la Atmósfera (CIMA/CONICET-UBA), Ciudad Universitaria, Pabellón II, 2do. Piso. (C1428EGA) Ciudad Autónoma de Buenos Aires, Argentina.

[3]Centro de Investigaciones del Mar y la Atmósfera (CIMA/CONICET-UBA), Ciudad Universitaria, Pabellón II, 2do. Piso. (C1428EGA) Ciudad Autónoma de Buenos Aires, Argentina.

[4]Centro de Investigaciones del Mar y la Atmósfera (CIMA/CONICET-UBA), Ciudad Universitaria, Pabellón II, 2do. Piso. (C1428EGA) Ciudad Autónoma de Buenos Aires, Argentina.

[5]Servicio de Hidrografía Naval and ESCM-INUN, Av. Montes de Oca 2124 (C1270ABV) Ciudad Autónoma de Buenos Aires, Argentina.

[6]Departamento Ciencias de la Atmósfera y los Océanos, Facultad de Ciencias Exactas y Naturales, Universidad de Buenos Aires, Ciudad Universitaria, Pabellón II, 2do. Piso. (C148EGA) Ciudad Autónoma de Buenos Aires, Argentina.

Note. Discussion open until February 1, 2009. Separate discussions must be submitted for individual papers. The manuscript for this technical note was submitted for review and possible publication on April 27, 2006; approved on June 15, 2007. This technical note is part of the ***Journal of Waterway, Port, Coastal, and Ocean Engineering***, Vol. 134, No. 5, September 1, 2008. ©ASCE, ISSN 0733-950X/2008/5-299–305/$25.00.

ered, data records are not long enough to build a wave climate. Finally, global wave models do not have enough resolution to provide reliable wave parameters at the intermediate and upper RDP.

For these reasons, at present, a realistic wave climate in the RDP and adjacent continental shelf can only result from the implementation of a numerical model system forced by wind data from a reliable database (at least 30 years long). The main limitation for wave climate modeling in the RDP has been the deficiency of observations of atmospheric variables in the region. Given the lack of historical direct wind observations over the estuary and the adjacent continental shelf and the low temporal resolution and short time span of satellite wind data, studies of wind variability (Simionato et al. 2005) and sea surface elevation hindcasting (Simionato et al. 2006) in the region have been mostly based on data/model derived products such as the reanalyses of the National Center for Environmental Prediction/National Center for Atmospheric Research (NCEP/NCAR) (Kalnay et al. 1996).

The aim of this note is to implement a wind wave numerical model for the RDP and the adjacent continental shelf, which will be used to study the wave climate in the region. The Simulating WAves Nearshore (SWAN) model has been selected for application in this case given that it has undergone significant testing—perhaps the most extensive testing of any shallow-water wave model—and it is successfully applied (internationally) by more than 100 users (Allard et al. 2002). The capability of this model forced by the NCEP/NCAR reanalyzed 10 m winds—data available from January 1, 1948 to the present—to reproduce observed wave parameters in the outer RDP is assessed by the quantification of the differences between simulated wave parameters and direct wave observations gathered at the mouth of the estuary.

Model Description

SWAN Model Description

SWAN is a numerical wave model that provides realistic estimates of wave parameters in coastal areas (Booij et al. 1999; Ris et al. 1999). Even though this model was specifically designed for coastal applications, it can be applied to wind generated surface gravity waves on any scale (Holthuijsen et al. 2004). The model is based on the wave action balance equation. The spectrum considered is the action density spectrum rather than the energy density spectrum since in the presence of currents, action density is conserved; whereas, energy density is not (e.g., Whitham 1974). A detailed explanation about the formulation of wind input, dissipation (whitecapping, bottom friction, and depth-induced breaking) and nonlinear wave–wave interaction terms can be seen in Holthuijsen et al. (2004). The frequency space generated in the numerical experiments presented in this note has 20 frequencies, between 0.05 and 1.00 Hz. The SWAN model is initialized at rest, wave parameters are set to zero at every grid point. Using this initial condition the first wave parameter fields can be quite misleading, so, the first two days in all the numerical simulations were disregarded.

Hydrodynamic (WQMap) Model Description

The hydrodynamic model used for generating current and sea level fields is Water Quality Mapping (WQMap) version 5.0, developed by Applied Science Associates Inc. (2004). The mathematical description of wind/tide driven currents requires the simultaneous solution of the dynamic momentum and continuity equations. It was assumed that vertical accelerations are negligible (pressure is hydrostatic over depth) and that fluid density is homogeneous. The two-dimensional vertically averaged momentum and continuity equations are solved. The bottom stress is parameterized by means of a quadratic law in terms of the depth averaged current velocity. A constant friction coefficient equal to 0.003 was selected for the numerical experiment described in this notes. The model is initialized at rest, currents and sea levels set to zero at every grid point. Both atmospheric and tidal forcing are then included in the simulations. WQMap uses a quadratic wind stress formulation with a constant wind stress coefficient (0.0014). Tides were introduced by imposing tidal elevation at the open boundaries using amplitudes and phases derived from the Oregon State University global model (Egbert et al. 1994). A water discharge of 22,000 m^3/s was included at the corresponding node in the upper part of the estuary.

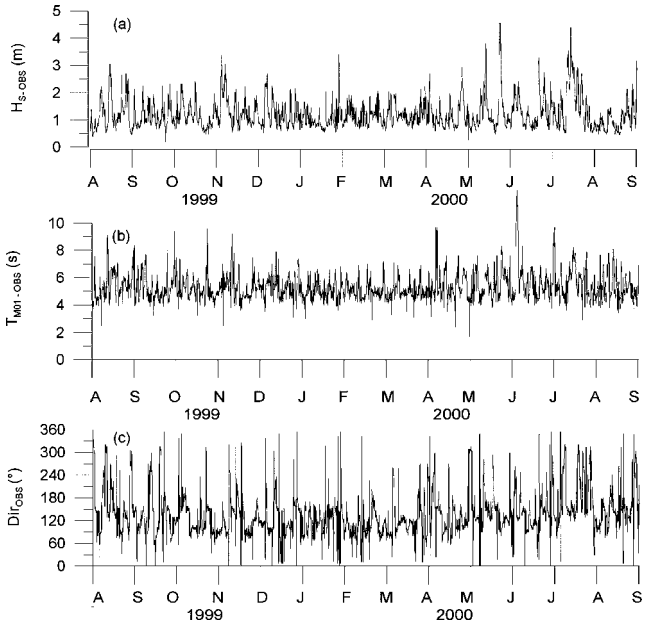

Fig. 2. Wave parameters observed at the mouth of the RDP. Data series of (a) significant wave heights; (b) mean periods; and (c) wave directions.

Data

Waves

The only in situ wave observations available in the RDP were collected between June 1996 and November 2001 using a Datawell Waverider directional wave recorder (Datawell 1997) moored in the outer estuary at 35° 40′S and 55° 50′W (Fig. 1). The instrument was programmed to measure 20 min sea level records with a 0.5 s sampling interval, every 2 h and 40 min. Data were retrieved during the aforementioned 5 year period with four gaps, 1, 5, 8, and 16 months long, respectively. Therefore, a total of 11,297 records (equivalent to 3 years) are valid.

The observed series of significant wave height (H_S), average periods (T_{M01}), and direction (α) for the period spanning August 1999 to August 2000—the only whole period of the record that does not present any gap—is shown in Fig. 2. It can be seen that

in the outer RDP significant heights are almost always greater than 0.5 m [Fig. 2(a)]. The minimum, maximum, and mean observed H_S (T_{M01}) are 0.18, 4.55, and 1.23 m (1.7, 10.7, and 4.8 s), respectively [Figs. 2(a and b)]. The mean observed wave direction [Fig. 2(c)] is 135.2°, corresponding to southeasterly as the most frequent direction of wave propagation. The frequency of occurrence calculated by Dragani and Romero (2004) indicates southeasterly, easterly, and southerly as the most frequent directions of propagation, corresponding to 41, 28, and 14% of the cases, respectively, whereas frequencies for the other directions are always equal to or less than 5%.

Wind

The atmospheric forcing for SWAN and WQMap models were the four daily fields (0, 6, 12 y, 18 GMT) of the wind components at 10 m from the NCEP/NCAR reanalyses. Reanalyses are not direct observations but the result of an objective analysis combining rawinsonde observations around the world, remote observations collected via satellite-borne instruments and a physical numerical model (Kalnay et al. 1996). The result of this analysis is a set of gridded data (spatial resolution: 1.875° in longitude, 1.905° in latitude) with a temporal resolution of 6 h. The main advantages of the reanalyses are their physical consistency and relatively high temporal coverage (since January 1, 1948 to the present). Full details of the NCEP/NCAR project and the dataset are given in Kalnay et al. (1996), and discussions about product quality over the Southern Hemisphere can be found in Simmonds and Keay (2000), among others. Bilinear (linear) interpolation was used to generate appropriate wind fields to match the spatial (temporal) resolution of the SWAN and WQMap models.

Bathymetry

The study area spans the region between 30°S and 42°S, and 40°W and 65.5°W, approximately and includes, therefore, regions as dissimilar as the very shallow RDP, the Uruguayan continental shelf, part of the adjacent Argentinean and Brazilian continental shelves, and a portion of the Southwestern Atlantic Ocean (Fig. 1). Bathymetry data for the models were obtained as a combination of a $1' \times 1'$ resolution depth dataset coming from GEBCO (2003) for the continental shelf and from digitalized nautical charts for the RDP (SHN 1986, 1992, 1993, 1999a, and 1999b). These data were interpolated to the model grid by applying the method of inverse distance to the power (with power equal to 2).

Results

Sensitivity to Model Domain and Resolution

A set of numerical experiments was run in which different domains, from a small one (shown by a dashed line in Fig. 1) to a very large one (covering an area larger than that shown in the figure) were tested for different resolutions. The smallest domain/largest resolution (with 138×90 grid points for resolutions of 2.7×3.3 km in the east–west and north–south directions, respectively) produced a mean-root-square error, E_{rms}, for heights equal to 0.41 m. The numerical experiments showed that a gradual reduction in E_{rms} results from the increase of the domain extension. After several simulations, it was found that the best grid corresponds to that shown by the whole area shown in Fig. 1 with a grid spacing of 22.7×20.0 km (100×70 grid points), for which E_{rms} was of 0.37 m. This value can be considered acceptable and is similar to those obtained for other regions. For instance, Dykes et al. (2002), who implemented SWAN for the northern Gulf of Mexico, obtained an E_{rms} of 0.30 m.

Table 1. Mean-Root-Square Error (E_{mrs}) and Bias between Observed and Modeled Wave Parameters, Obtained from Different Numerical Experiments

Numerical experiment	Height (m) E_{mrs}, *bias*	Period (s) E_{mrs}, *bias*	Direction (°) E_{mrs} *bias*
No C_D correction ($K=1$); no current	0.53, 0.41	2.7, 2.5	61, 17
$K_0=5.4$ m/s; no current	0.37, 0.13	1.5, 2.2	65, 17
$K_0=7.7$ m/s; no current	0.37, −0.03	2.3, 2.0	61, 16
$K_0=16.2$ m/s; no current	0.62, −0.39	2.0, 1.6	61, 16
Current and sea level fields; $K_0=7.7$ m/s	0.35, −0.08	2.4, 2.0	67, 8
Nested in Atlantic grid; $K_0=7.7$ m/s	0.37, −0.04	2.3, 2.0	61, 16

Note: The factor and the coefficient used to correct NCEP/NCAR wind speed are K and K_0, respectively [defined in Eq. (3)]. Only a selection of results has been included.

Sensitivity to Wind Drag

The SWAN model is driven by the wind speed at 10 m elevation, U, whereas the computations use friction velocity, U_*. For SWAN the transformation from U to U_* is obtained by

$$U_*^2 = C_D U^2 \tag{1}$$

in which C_D is the drag coefficient from Wu (1982) given by

$$1.2875 \times 10^{-3}, \quad U < 7.5 \text{ m/s}$$

$$C_D = (0.8 + 0.065U) \times 10^{-3}, \quad U \geqslant 7.5 \text{ m/s} \tag{2}$$

It has been shown that even though NCEP/NCAR reanalyses properly reproduce the observed wind direction in the RDP, they tend to underestimate wind speed, particularly for weak wind conditions (Simionato et al. 2006). Although simulated waves are proportional to the measured ones, simulated heights are too low when compared to observations, especially for weak winds. A set of sensitivity experiments was run to evaluate the coefficient (K) that must be applied to C_D in order to simulate the observed wave parameters. This factor K was chosen to depend on the wind speed U (similar to Simionato et al., 2006) and is expressed as follows:

$$K = 1 + e^{-U/Ko} \tag{3}$$

where Ko is a coefficient (with wind velocity units) that must be optimized. The corrected expression for C_D is given by

$$1.2875K^2 \times 10^{-3}, \quad U < 7.5 \text{ m/s}$$

$$C_D = (0.8 + 0.065KU)K^2 \times 10^{-3}, \quad U \geqslant 7.5 \text{ m/s} \tag{4}$$

This formulation will tend to keep the original values of C_D for strong winds but will introduce an increasingly larger correction as wind speed becomes smaller. Numerical sensitivity experiments using values of Ko ranging from 5.4 m/s (10 knots) to 16.2 m/s (30 knots) were run. Results are shown in Table 1. An acceptable E_{rms} and *bias* were found for Ko equal to 7.7 m/s

(14 knots). For this *Ko*, the *K* factor is almost duplicated for weak (near null) winds and is less than 1.3 when wind speed is more than 10 m/s. Note that the fact that NCEP/NCAR reanalyses underestimate weak winds, but better capture intense events is in agreement with wave model results for other areas. For instance, Qi et al. (2002), who used those reanalyses to model waves in the South China Sea, found that maximum differences between significant wave height from the WAVE WATCH model and TOPEX/POSEIDON data, occurred for low wind speeds. It must be clearly remarked that this factor is only recommended to correct NCEP/NCAR reanalyses when they are used to force the SWAN model in the RDP and adjacent continental shelf region.

An additional numerical experiment was run nesting the selected grid in a larger computational domain (spatial resolution: 0.71° in longitude, 0.55° in latitude), which spans from 15°S to 65°S and from 20°E to 70°W, covering almost all the South Atlantic Ocean. The SWAN model was also forced with NCEP/NCAR reanalysis data in this large domain, even though it is known that the use of SWAN (version 40.51) on oceanic scales is less efficient than WAVEWATCH III and probably less efficient than wave prediction model (WAM). Although it is known that the numerical diffusion could be fairly large in long propagation distances (oceanic scales) (Booij et al. 1999) this numerical experiment was only run in order to test the sensitivity of the results when boundary conditions are imposed. As there were no significant differences between E_{rms} and *bias*—with and without nesting the selected domain in the Atlantic one—it can be concluded that the selected domain is large enough to generate realistic wind wave fields (sea and swell) in the mouth of the RDP estuary (Table 1).

Sensitivity to Background Current and Sea Level Variations

The technique of linking a spectral wave model to a hydrodynamic model is an effective tool for wave prediction in estuaries (Chen et al. 2005). At the mouth of the RDP, maxima tidal ranges decrease from 1.55 m at San Clemente (Argentina) to 0.40 m at Punta de Este (Uruguay), and maximum tidal current is lower than 0.3 m/s (SHN, 2007; Simionato et al., 2004). In order to test the sensitivity of the model-data agreement to the inclusion (or omission) of the background current and sea level variations, hydrodynamic fields derived from WQMap were included in the simulations. It can be seen (Table 1) that simulated wave parameters in the outer RDP do not significantly improve after including the current and sea level field in the computational domain. In fact, E_{rms} is reduced from 0.37 to 0.35 m, and the absolute value of *bias* is slightly enlarged from 0.03 to 0.08. Therefore, it was decided not to include the current and sea level fields as hydrodynamic conditions in further simulations with the SWAN model.

Selected Modeling Architecture: Validation

Differences between simulated and observed wave parameters are given in Fig. 3. Computed E_{rms} for H_S, T_{M01}, and α are 0.37 m, 2.3 s, and 61°, respectively, and computed *bias* are of −0.03 m, 2.0 s, and 16°, respectively (Table 1). A dispersion diagram between the 3,596 observed and simulated wave heights and directions are shown in Fig. 4, where very good agreement is evident; the linear determination coefficient, r^2, is 0.93 and 0.82, respectively. Direction differences of more than 100° are almost always associated with simulated wave heights less than 0.2 m [these directions are mainly located outside the sector formed by the dashed lines with slopes equal to 0.5 and 2, Fig. 4(b)]. The SWAN model slightly underpredicted T_{M01} with a fairly large scatter and low determination coefficient. It is consistent with results obtained by Lin et al. (2002) who applied the SWAN model in the

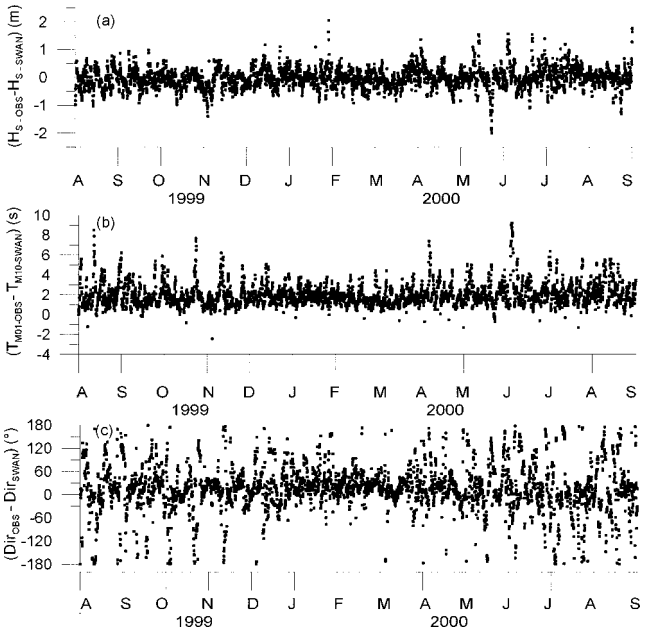

Fig. 3. Differences between observed and simulated wave parameters: (a) significant wave heights; (b) mean periods; and (c) wave directions

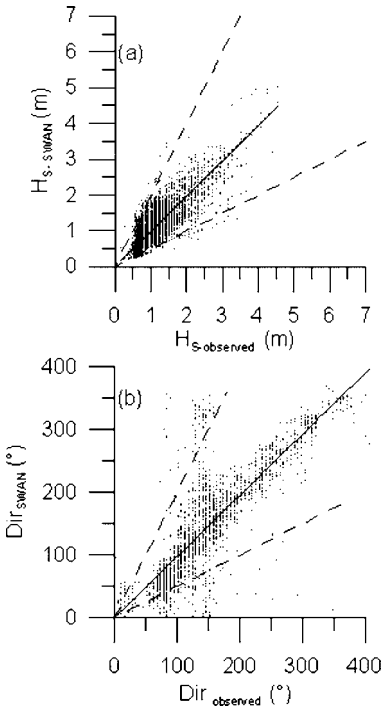

Fig. 4. Scatter plot of measured versus simulated (a) significant wave heights, based on 3,596 observations and (b) directions, corresponding to high-energy conditions (events with significant wave heights lower than 1 m are not included). Solid line represents the best adjustment obtained from the least-root-square method. Dashed lines with slopes equal to 0.5 and 2 are included as references.

Table 2. Monthly and Total Mean-Root-Square Error (E_{mrs}), Bias, and Determination Coefficient (r^2) between Observed and Modeled Wave Parameters from August 1999 to August 2000

Month	E_{mrs} (m, s, °) H, T, direction	*Bias* (m, s, °) H, T, direction	r^2 H, direction
August 1999	0.38, 2.6, 80	−0.07, 2.2, 17	0.93, 0.80
September 1999	0.33, 0.3, 64	−0.07, 2.0, 11	0.93, 0.84
October 1999	0.38, 2.0, 51	−0.19, 1.7, 6	0.95, 0.85
November 1999	0.33, 2.2, 55	−0.06, 1.9, 11	0.95, 0.82
December 1999	0.32, 2.2, 57	0.04, 2.0, 21	0.94, 0.80
January 2000	0.36, 2.0, 53	0.00, 9, 34	0.90, 0.77
February 2000	0.29, 1.8, 45	−0.07, 1.6, 26	0.95, 0.86
March 2000	0.34, 2.2, 62	−0.04, 1.9, 25	0.91, 0.87
April 2000	0.28, 2.3, 70	−0.09, 2.0, 27	0.96, 0.87
May 2000	0.55, 2.9, 66	0.03, 2.3, 13	0.90, 0.81
June 2000	0.42, 2.5, 79	0.02, 2.2, 18	0.90, 0.79
July 2000	0.37, 2.3, 69	0.11, 2.1, −5	0.96, 0.91
August 2000	0.38, 2.7, 80	−0.02, 2.3, 18	0.89, 0.79

Chesapeake Bay and obtained a slight underestimation in simulated periods.

The monthly variation of E_{rms}, *bias*, and r^2 for wave parameters are shown in Table 2. E_{rms} ranges from 0.28 to 0.55 m, 0.3 to 2.9 s, and 45° to 80° for H_S, T_{M01}, and α, respectively, *bias* from −0.19 to 0.11 m, 1.6 to 2.3 s, and −5° to 34° for H_S, T_{M01}, and α, respectively, and r^2 from 0.89 to 0.95 and 0.77 to 0.91 for H_S and α, respectively. In general, results are satisfactory for every month of the year.

This validated regional coarse wave model constitutes the basis for developing a climate wave study in the region. In this sense, some encouraging preliminary results were obtained—not included in this technical note—nesting an intermediate resolution (6×6 km) SWAN model for the RDP to the validated one. Preliminary sensitivity numerical experiments reveal the necessity to include sea level and current fields in the upper and intermediate (shallow) RDP because their effects have been shown to be very significant there. Finally it is central to stress the importance and need of in situ wave observations in the upper and intermediate parts of the RDP estuary to allow more and better scientific studies leading to appropriate knowledge of this important phenomenon.

Case Study

The most energetic wave event measured at the outer RDP was simulated, and the estimated wave parameters were compared with observations. On May 16, 2000, a low pressure system with very intense winds over the RDP estuary, produced floods, damage, and fatalities in the region. The synoptic evolution of this "superstorm" over eastern Argentina from May 14 to May 17 has been studied using conventional observations and six hourly operational NCEP analyzed datasets (Possia et al. 2003). On May 16

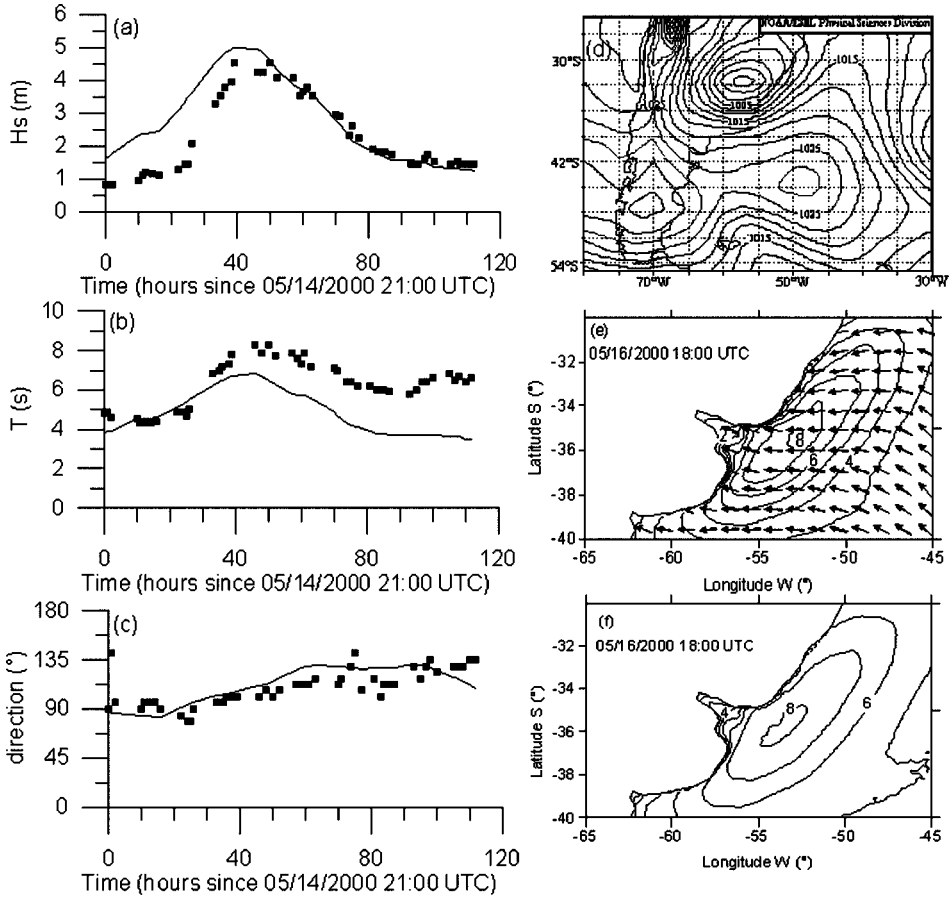

Fig. 5. Case study: May, 2000. Series of observed (dot) and simulated (line) (a) height; (b) period and (c) direction; (d) synoptic situation (May 16, 12 UTC), instantaneous (e) height (m) and direction fields; and (f) period field.

(Fig. 5(d)), the cyclonic system acquired a closed vertical structure over the RDP, with a closed isobar of 999 hPa at the surface producing very intense and persistent southeasterly winds of 18 m/s and gusts reaching 30 m/s. Fig. 5 shows good agreement between observed and simulated wave heights [Fig. 5(a)] and directions [Fig. 5(c)] and a slight underprediction, lower than 2 s, for simulated periods [Fig. 5(b)]. Instantaneous wave parameter fields are shown in Fig. 5(e) (heights and directions) and Fig. 5(f) (periods).

Conclusions

Numerical experiments show that the relatively low resolution SWAN model implemented in this note—forced by NCEP/NCAR wind reanalysis—simulates lower wave heights than the ones observed, especially for weak winds. So, after some numerical experiments, a correction factor was applied to the wind drag coefficient in order to minimize the E_{rms} and *bias* between simulated and observed wave parameters. The agreement between simulated and observed *Hs* and α is very satisfactory, but the simulated T_{M01} are slightly underestimated in, approximately, 2 s. The most intense wave event observed in the RDP mouth was satisfactorily simulated using the modeling architecture described.

Acknowledgments

This note is a contribution to the PICT 2002 07-12246 Project "Estudio de la dinámica oceánica y atmosférica del estuario del Río de la Plata mediante un sistema de modelado numérico integral," PICT 2005 32606 Project "Variabilidad climática en el Río de la Plata. Cambios en los climas de olas, niveles, transportes y posición y estructura de la cuña salina durante los últimos 50 años y respuesta a potenciales escenarios futuros" and the UBA Grant No. X264.

Notation

The following symbols are used in this technical note:

C_D = drag coefficient;
E_{rms} = mean-root-square error;
H_S = significant wave height;
K = factor to be applied to the drag coefficient;
K_o = coefficient to be optimized;
T_{M01} = average wave period;
U = wind speed;
U_* = friction velocity; and
α = wave direction.

References

Allard, R. A., Kaihatu, J., Hsu, Y. L., and Dykes, J. D. (2002). "The integrated ocean prediction system (IOPS): Special issue—Navy operational models: Ten years later." *Oceanogr.*, 15(1), 67–76.

Applied Science Associates Inc. (2004). *Wqmap user's manual*, version 5.0, Applied Sci. Assoc., Narragansett, R.I.

Booij, N., Ris, R. C., and Holthuijsen, L. H. (1999). "A third-generation wave model for coastal regions. 1: Model description and validation." *J. Geophys. Res.*, 104(c4), 7649–7666.

Chen, Q., Zao, H. H., Hu, K., and Scott, D. L. (2005). "Prediction of wind waves in a shallow estuary." *J. Waterway, Port, Coastal, Ocean Eng.*, 131(4), 137–148.

Cotton, P. D., and Carter, D. J. T. (1994). "Cross-calibration of TOPEX, ERS-1, and Geosat wave heights." *J. Geophys. Res.*, 99(C12), 25025–25033.

Cox, A. T., and Swail, V. R. (2001). "A global wave hindcast over the period 1958–1997: Validation and climatic assessment." *J. Geophys. Res.*, 106(C2), 2313–2329.

Datawell. (1997). *Manual for the waverider*, Laboratory for Instrumentation, LM Haarlem, The Netherlands.

Dobson, E., Maldonado, F., and Goldhirsh, J. (1987). "Validation of Geosat altimeter-derived wind speeds and significant wave heights using buoy data." *J. Geophys. Res.*, 92(10), 10719–10731.

Dragani, W. C., and Romero, S. I. (2004). "Impact of a possible local wind change on the wave climate in the upper Río de la Plata." *J. Climatol.*, 24(9), 1149–1157.

Dykes, J. D., Hsu, L., and Rogers, W. E. (2002). "SWAN evaluation in the northern Gulf of Mexico." *7th Int. Workshop on Wave Hindcasting and Forecasting*, Banff, Alberta, Canada.

Egbert, G. D., Bennett, A. F., and Foreman, M. G. G. (1994). "TOPEX/POSEIDON tides estimated using a global inverse model." *J. Geophys. Res.*, 99(C12), 24821–24852.

GEBCO. (2003). *User's guide to the centenary edition of the GEBCO digital atlas and its data sets*, M. T. Jones, ed., Natural Environment Research Council.

Gulev, S. K., Grigorieva, V., Sterl, A., and Woolf, D. (2003). "Assessment of the reliability of wave observations from voluntary observing ships: Insights from the validation of a global wind wave climatology based on voluntary observing ship data." *J. Geophys. Res.*, 108(C7), 3236.

Holthuijsen, L. H., et al. (2004). *Swan cycle III version 40.31, user's manual*, Delft Univ. of Technology, Faculty of Civil Engineering and Geosciences, Environmental Fluid Mechanics Section, Delft.

Kalnay, E., et al. (1996). "The NCEP/NCAR 40-year reanalisis project." *Bull. Am. Meteorol. Soc.*, 77(3), 437–471.

Lin, W., Sandford, L. P., and Suttles, S. E. (2002). "Wave measured and modeling in Chesapeake Bay." *Continental Shelf Res.*, 22(18), 2673–2683.

Possia, N., Cerne, S. B., and Campetella, C. (2003). "A diagnostic analysis of the Río de la Plata, May 2000." *Meteorl. Appl.*, 10(1), 87–99.

Qi, Y., Chu, P. C., and Shi, P. (2002). "Comparison of significant wave height from wave-watch model and topex/poseidon data." *8th OMISAR Workshop on Ocean Models*, Hong Kong.

Ris, R. C., Holthuijsen, L. H., and Booij, N. (1999). "A third-generation wave model for coastal regions. 2: Verification." *J. Geophys. Res.*, 104(c4), 7667–7681.

SHN. (1986). *Mar Argentino, de Río de la Plata al Cabo de Hornos*, Nautical Chart, 50, 4th Ed., Servicio de Hidrografia Naval, Armada Argentina.

SHN. (1992). *Acceso al Río de la Plata*, Nautical Chart H1, 5th Ed., Servicio de Hidrografia Naval, Armada Argentina.

SHN. (1993). *El Rincón, Golfo San Matías y Nuevo*, Nautical Chart H2, 4th Ed., Servicio de Hidrografia Naval, Armada Argentina.

SHN. (1999a). *El Río de la Plata Medio y Superior*, Nautical Chart H116, 4th Ed., Servicio de Hidrografia Naval, Armada Argentina.

SHN. (1999b). *Río de la Plata Exterior*, Nautical Chart H113, 2nd Ed., Servicio de Hidrografia Naval, Armada Argentina.

SHN. (2007). *Tablas de Marea 2007*, H-610, Servicio de Hidrografía Naval, Armada Argentina.

Simionato, C., Dragani, W., Nuñez, M., and Engel, M. (2004). "A set of 3-D nested models for tidal propagation from the Argentinean continental shelf to the Río de la Plata estuary. Part I: M_2." *J. Coastal Res.*, 20(3), 893–912.

Simionato, C., Meccia, V., Dragani, W., and Nuñez, M. (2006). "On the use of the NCEP/NCAR surface winds for modeling barotropic circulation in the Río de la Plata estuary." *Estuarine, Coastal and Shelf Sci.*, 70(1–2), 195–206.

Simionato, C., Vera, C., and Siegismund, F. (2005). "Surface wind variability on seasonal and interannual scales over Río de la Plata area." *J. Coastal Res.*, 21(4), 770–783.

Simmonds, I., and Keay, K. (2000). "Mean southern hemisphere extratropical cyclone behavior in the 40-year NCEP-NCAR reanalysis." *J. Clim.*, 13(5), 873–885.

Sterl, A., Komen, G. J., and Cotton, D. (1998). "Fifteen years of global wave hindcasts using winds the European Centre for Medium-Range Weather Forecasts reanalysis: Validating the reanalyzed winds and assessing the wave climate." *J. Geophys. Res.*, 103(C3), 5477–5492.

Whitham, G. B. (1974). *Linear and nonlinear waves*, Wiley, New York.

Wilkerson, J. C., and Earle, M. D. (1990). "A study of differences between environmental reports by ships in the voluntary observing program and measurements from NOA buoys." *J. Geophys. Res.*, 95(c3), 3373–3385.

Woolf, D. K., Challenor, P. C., and Cotton, P. D. (2002). "Variability and predictability of the North Atlantic wave climate." *J. Geophys. Res.*, 107(C10), 3145 .

Wu, J. (1982). "Wind-stress coefficients over sea surface from breeze to hurricane." *J. Geophys. Res., C: Oceans Atmos.*, 87(C12), 9704–9706.